Prompt multigluon production in high-energy collisions from singular Yang-Mills solutions

Romuald A. Janik
The Niels Bohr Institute, Blegdamsvej 17, DK-2100 Copenhagen, Denmark
and M. Smoluchowski Institute of Physics, Jagellonian University, Reymonta 4, 30-059 Cracow, Poland

Edward Shuryak and Ismail Zahed
Department of Physics and Astronomy, State University of New York, Stony Brook, New York 11794
(Received 13 June 2002; published 16 January 2003)

Nonperturbative parton-parton scattering is studied using the Landau method. Specific singular O(3)-symmetric solutions to the Euclidean Yang-Mills equations are discussed, with instanton dynamics incorporated in the overlap between incoming and vacuum fields. We derive a high-energy solution at small times, and assess the gluonic state produced at the turning point (escape point to Minkowski space-time). We follow the solution as it escapes to Minkowski space and assess its *outgoing* gluon spectrum. The solution is found to follow from the Yang-Mills sphaleron problem studied recently through a simple rescaling. We also argue, by evaluating the number of *incoming* gluons for the same singular solution, that this scaling is in fact more general and presumably describes the energy dependence of the spectra and multiplicities at *all* energies.

DOI: 10.1103/PhysRevD.67.014005 PACS number(s): 12.38.Mh

I. INTRODUCTION

Tunneling phenomena related to the topology of Yang-Mills fields are described semiclassically by instantons [1,2]. Some manifestations of these effects related to explicit breaking of U(1) and spontaneous breaking of SU(N_f) chiral symmetries are by now understood in significant detail due to strong ties to hadronic phenomenology and lattice studies (see, e.g., [3] for a review).

We know much less about their role in the cross section of various high-energy reactions. Such studies got a big boost in the early 1990s, when *baryon-number violating* instanton-induced processes of the electroweak theory were actively discussed [4–6]. These developments were generalized to hard processes in QCD through small size instantons, and there are current attempts to see their contribution to multijet production at the DESY ep collider HERA (for a recent review see [7]).

Recently [8,9] it was suggested that nonperturbative configurations composed of an instanton or anti-instanton play an important role in parton-parton scattering amplitudes at high energy, and may account for most of the soft Pomeron slope and intercept. The logarithmic rise of the inelastic cross section was shown to follow from coherent multiple gluon production as described by the semiclassical field following from an interacting instanton–anti-instanton configuration. This mechanism was shown to be the same for pp and $\bar{p}p$ [8]: so no odderon appears in the classical limit.

At low energy transfer in the center of mass, the interaction is dipolar, and accounts for the rise in the partial cross section from first principles. At intermediate and large energy transfer, the dipole approximation is not reliable as strong instanton–anti-instanton interactions set in together with unitarity constraints [5,8]. Unlike perturbative processes, for which the production of each subsequent gluon is associated with a power of the small coupling constant, in instanton-induced processes the cross section rises with the number of gluons produced, reaching a maximum at some parametrically large value $N \sim 1/\alpha(\rho)$. The physical reason for this is that particular *coherent clusters* of the gauge field are actually produced, instead of independent gluons. In a recent paper [10] properties of minimal clusters of this kind were discussed: the clusters themselves were identified via constrained minimization of the Yang-Mills energy, with fixed size and Chern-Simons number, and their subsequent real time evolution has been studied both numerically and analytically.

However, in real collisions the Yang-Mills energy or action of the final state is only one of the contributing factors. Another crucial factor is the *overlap* between the initial system of colliding gluons and the instanton, or whatever the tunneling path is. One way [11] to include both factors together from first principles, and also enforce the unitarity constraints, is to use a semiclassical approximation to the partial cross section based on an adaptation of the Landau formula for overlapping matrix elements in terms of singular field configurations. The occurrence of a singularity is an essential feature of the Euclidean field configuration that interpolates between the vacuum at $t=-\infty$ with zero energy, and the escape point at $t=0$ with finite energy.

By following this ''Landau method,'' as it was called by Diakonov and Petrov [12], these authors were able not only to get the known low-energy limit of the amplitude, but also to assess the high-energy one. Although they did not solve for the field configuration at small times explicitly, they were still able to obtain the corresponding action and other quantities and thus were able to predict the behavior of the cross section at high energies. Comparing both limits has confirmed that the cross section has a maximum near the sphaleron energy, and that its value is close to the square root of the original low-energy tunneling amplitude.

The aim of our paper is to analyze further the singular gauge configurations at the *escape time* $t=0$. We start with the high-energy limit following [12] and show how one can find the turning (or escape) point field configuration, describing the cluster produced at $t=0$. It turns out that this con-

 ©2003 The American Physical Society

figuration can be related to the minimal QCD sphaleron [10] by a particular *scaling law*, containing a power of Q/M_s. We then show that the subsequent evolution (explosion) in real time of these clusters can also be obtained by our rescaling, generalizing recent work [10]. The resulting spectrum of gluons and their multiplicity can then be obtained. We then argue that the prescribed scaling law is valid not only at high energies, above the sphaleron mass, but in fact at *all* energies.

In Sec. II we recall standard notation for the spherically symmetric gauge configurations used. In Sec. III, we recall the main approaches to evaluating the inelastic parton-parton scattering in the eikonal approximation. In Sec. IV, we show that the singular gauge configurations at the escape points follow from the sphaleron point for all energies through a pertinent rescaling, which is our main result. In Sec. V, we assess the number of incoming and outgoing gluons per sphaleron for fixed center of mass energy in the semiclassical approximation. The Appendices contain a number of useful results including a stability analysis of the escaping configurations under perturbative light pair decay.

II. O(3)-SYMMETRIC YANG-MILLS

We consider the QCD Yang-Mills (YM) theory wherein all dimensions are rescaled away by the sphaleron (antisphaleron) mass M_S,

$$M_S=\frac{1}{4\alpha}\int_0^\infty dx x^2 \frac{96\rho^4}{(x^2+\rho^2)^4}=\frac{3\pi}{4\alpha\rho}, \tag{1}$$

unless specified otherwise. In the vacuum $\alpha\approx 0.7$, $\rho\approx 1/3$ fm,[1] with typically $M_S\approx 2$ GeV. In the scattering process, the sphaleron (antisphaleron) size ρ may change. We work mainly in the temporal gauge. The YM potential **V**, kinetic energy **K**, and Chern-Simons number **N** are

$$\mathbf{V}=\frac{M_S}{4\pi\alpha}\int d\vec{x}\frac{1}{4}(F^a_{ij})^2,$$

$$\mathbf{K}=\frac{M_S}{4\pi\alpha}\int d\vec{x}\frac{1}{2}(\dot{A}^a_i)^2,$$

$$\mathbf{N}=\frac{1}{16\pi^2}\int d\vec{x}\,\epsilon_{ijk}\left(A^a_i\partial_j A^a_k+\frac{1}{3}\epsilon_{abc}A^a_iA^b_jA^c_k\right), \tag{2}$$

where we have ignored quarks for simplicity.

In parton-parton scattering with large $\sqrt{s}$, the incoming kinematics boils down to an eikonalized cross section as in Eq. (8) with a partial cross section $\sigma(Q)$ with $Q\approx M_S\ll\sqrt{s}$. In the center of mass it is reasonable to consider the gluonic configurations that maximize $\sigma(Q)$ to possess higher symmetries than completely arbitrary fields.[2] Here we take them to have spherical O(3) symmetry of the sphaleron

$$A^a_i(\vec{x},t)=+\epsilon_{aij}n_i[1-A(x,t)]/x + (\delta_{ai}-n_an_i)B(x,t)/x+n_an_iC(x,t)/x \tag{3}$$

where $n_i=\vec{x}_i/x$ is a unit three-vector, and $|\vec{x}|=x\geqslant 0$ a radial variable. Since we are interested in singular gauge fields, we assume the three two-dimensional independent functions A,B,C to be continuous and differentiable everywhere in Euclidean space, except at $x=0$ where a singularity will be located for fixed times $\pm T/2$. In terms of Eq. (3) the Euclidean action

$$S=\int dt(\mathbf{K}+\mathbf{V}) \tag{4}$$

reads

$$S=\frac{1}{\alpha}\int dt\int_0^\infty dx\left(\dot{A}^2+\dot{B}^2+\frac{1}{2}\dot{C}^2+A'^2+B'^2 + \frac{(A^2+B^2-1)^2}{2x^2}+\frac{C^2(A^2+B^2)}{x^2}+\frac{2C(A'B-AB')}{x}\right) \tag{5}$$

where the time variable has been rescaled through $tM_S\to t$ in Eq. (5). The integration interval is to be specified below in the presence of a time singularity. Note that the energy

$$-Q=\mathbf{K}-\mathbf{V} \tag{6}$$

where in Euclidean space $-\mathbf{V}$ plays the role of the potential. For self-dual configurations $Q=0$. The Chern-Simons number is

$$\mathbf{N}=\frac{1}{2\pi}\int_0^\infty dx\left(A'B-B'A+\frac{C}{x}(A^2+B^2-1)\right). \tag{7}$$

The dual to the O(3) ansatz used here that maps on the antisphaleron follows similar reasoning and results as shown in Appendix A. The difference is a negative **N**.

[1] As discussed, e.g., in the review [3], lattice studies indicate that the instanton size distribution has a sharp peak around this value. At small ρ it happens because the semiclassical barrier becomes higher, while suppression at large ρ is not well understood. In this work we found that the effective size is reduced with increasing energy, making the suppression mechanism irrelevant.

[2] We expect that the sudden deposition of energy from the parton collision does not allow time for a change in the topological coordinates. That is, if in the vacuum there was a virtual configuration under the barrier with some Chern-Simons number, the one produced would be *on* the barrier with the same coordinate. We assume it to be spherical because (i) such clusters are relatively small objects, and (ii) spherical turning points are the only ones analytically tractable.

III. THE EVOLVING VIEWS ON NONPERTURBATIVE HIGH-ENERGY PROCESSES

In this work we discuss the so called semihard parton-parton processes, at fixed $\sqrt{-t}\sim 1$ GeV$\ll\sqrt{s}$, which involve certain nonperturbative QCD gauge configurations related to topological tunneling.

The original approach [4–6] we followed in [8] was based on the semiclassical instanton solution in the amplitude. To leading order in a small tunneling diluteness factor containing the instanton density and their typical size $\kappa = n_{inst}\rho^4 \sim 10^{-2}$ (see, e.g., [3] for details) the inelastic cross section was written as

$$\sigma_{IN}(s,t)\approx \mathbf{C}\pi\rho^2 \ \ln s \int dq_{1\perp}dq_{2\perp}\mathbf{K}(q_{1\perp},q_{2\perp},t) \times \int_{(q_{1\perp}+q_{2\perp})^2}^{\infty} dQ^2\kappa^2\mathbf{B}(Q) \tag{8}$$

where $\mathbf{K}$ is the pertinent instanton form factor at fixed $-t \ll s$, containing through-going partons in the form of Wilson lines. The square of κ appears because the amplitude is squared. $\mathbf{B}(Q)$ is the partial multigluon cross section for fixed $Q^2\ll s$ and $\mathbf{C}$ an overall constant which accounts for both the instanton and anti-instanton contributions to the initial state. To exponential accuracy

$$\kappa^2\mathbf{B}(Q)\approx \mathrm{Im}\int dT e^{QT-\mathbf{S}(T)} \tag{9}$$

where $\mathbf{S}(T)$ is the effective action describing the instanton–anti-instanton interaction for a time separation T, which is defined at large T to become twice the free instanton action. This effective action, also known as the ''holy grail function,'' is supposed to sum up contributions of *any* number of produced gluons. For small Q or large T, the dipole approximation is valid and Eq. (9) rises exponentially with Q [4]. However, as emphasized first by Zakharov [5] the unitarity constraints on the partial cross section require $\mathbf{B}(Q)$ to fall at large Q. Shifman and Maggiore [6] argued that the unitarization could be qualitatively enforced by resumming chains of instantons and anti-instantons. In [8] we followed this idea and indeed found that the dominant contribution to Eq. (9) occurs at the sphaleron point for which $\mathbf{B}(M_S)\approx 1/\kappa$. Hence,

$$\sigma_{IN}(s,t)\approx \mathbf{C}\pi\rho^2\kappa \ln s \int dq_{1\perp}dq_{2\perp}\mathbf{K}(q_{1\perp},q_{2\perp},t). \tag{10}$$

The rise in the partial inelastic cross section due to the production of the QCD sphaleron[3] results in an increase of the inelastic cross section by one power of the diluteness factor κ, or about a 100-fold increase [8].

This qualitative solution of the problem implies, however, that the maximal cross section does not correspond to a well-separated instanton–anti-instanton pair, but rather to a different field configuration, a close pair with $T\sim\rho$ with half the action annihilated. Detailed studies of close instanton–anti-instanton configurations have been made recently in [10], with the $t=0$ point describing the escape point (turning point) in Minkowski space of the gauge field configuration. Although this paper does not deal with the cross section calculation, one could in principle do so by modifying the form factor $\mathbf{K}$ in Eq. (1) using Wilson lines in half the instanton–anti-instanton field as described, e.g., by the Yung ansatz.

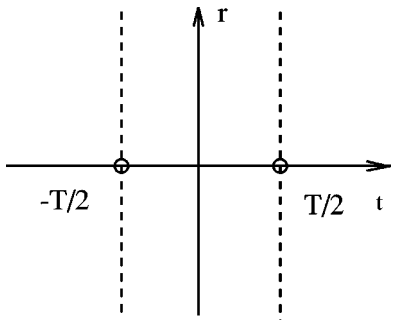

FIG. 1. The space distance–time $r-t$ plane. Small circles show the positions of the singularities; the vertical dashed lines indicate lines at which two solutions with different energies are joined together.

However, even this solution of the problem is not yet ideal, as it still treats two small semiclassical factors involved, the instanton–anti-instanton interaction $\mathbf{S}$ in the vacuum and the form factor $\mathbf{K}$ independently. The idea behind the Landau method is to combine both in one common semiclassical treatment. We do not repeat all the explanations and technical details the reader can find in [12], but just recall the main idea. Considering the quantum-mechanical overlap between the ground and highly excited states with energy Q, Landau wrote it as the difference of the shortened action for both paths, with energy 0 and Q, respectively. Naturally, the integral goes from the turning points to infinity. The singularity of the gauge configuration plays the role of such an infinity for the quantum coordinates. Specific Euclidean paths, used following [11,12], have singularities in the A_μ field located at $r=0$ and time $\mp T/2$ (see Fig. 1). Outside the region marked by the dashed lines the solutions are the universal singular instantons describing the ground state. Between the dashed lines it is supposed to be the (so far missing) energy-Q solution: the two join smoothly at the dashed lines. Our aim is to find the solution, at least approximately, and look at the $t=0$ plane, describing the turning states. This analysis will eventually lead to predictions of what is actually produced in the collision.

IV. MORE DETAILS OF SINGULAR YANG-MILLS SOLUTIONS

A. Singular fields: $|t|>T/2$

The branch of the field that interpolates between the vacuum at $t=-\infty$ and the singularity at $t=-T/2$ with zero energy and minimizes Eq. (4) is an instanton. The conjugate

[3]Of course, there is also production of the QCD antisphaleron, which carries the opposite Chern-Simons number.

branch is an anti-instanton and interpolates between the singularity at $t=+T/2$ and the vacuum at $t=+\infty$. In covariant gauge, both branches are given by

$$A^a_\mu(x(\pm))=2\,\eta_{\mu\nu}(\pm)x_\nu(\pm)\Phi(x^2(\pm))$$

$$=\frac{2\,\eta^a_{\mu\nu}(\pm)x_\nu(\pm)\rho^2}{[\rho^2-x^2(\pm)]x^2(\pm)} \tag{11}$$

where the $-$ field refers to the $t<-T/2$ time branch, and the $+$ field refers to the $t>T/2$ time branch, with

$$x(\pm)_\nu=(\vec{x},t_\pm)_\nu=(\vec{x},t\mp T/2\pm\rho)_\nu. \tag{12}$$

The 't Hooft symbols are identified as $\eta(+)=\eta(\text{anti-instanton})$ and $\eta(-)=\overline{\eta}(\text{instanton})$. For $|t|>T/2$ Eqs. (11) are singular self-dual solutions to the QCD Yang-Mills equations with zero energy. Note that the singularity in Eq. (11) stems from the change $\rho\to i\rho$ in the self-dual O(4) instanton. $A(+)$ is the time conjugate of $A(-)$.

The axial gauge $A_4=0$ is commensurate with the O(3) symmetry, and the results for the $\pm$ branches follow by using the hedgehog gauge transformation

$$U(\vec{x},t)=\exp\left(i\vec{x}\cdot\vec{\tau}\int^t dt'\Phi(\vec{x}^2+t'^2)\right), \tag{13}$$

modulo static gauge transformations. Under the action of Eq. (13) the A_4 part in the Lorentz gauge (11) is gauged to zero. The residual static gauge transformations are fixed by fixing the positions of the singularities in the axial gauge to coincide with those in the Lorentz gauge at $t=\mp T/2$. In particular,

$$A^a_i(\vec{x},-T/2)=A^a_i(\vec{x},+T/2)$$

$$=-(\epsilon_{aij}x_j+\delta_{ai}\rho)\frac{2\rho^2}{x^2(x^2+\rho^2)}. \tag{14}$$

B. Singular fields: $|t|<T/2$

The gauge configuration in the time interval $|t|<T/2$ follows from the YM equations using Eq. (14) as the singular boundary conditions. They are no longer constrained by self-duality, and hence carry finite energy Q. Fixed Q relates to fixed T through $Q=dS/dT$ where S is the Yang-Mills action in the time interval $|t|\leqslant T/2$.

1. Above the sphaleron

For small Euclidean times $T/\rho\ll 1$ or large energy, the singular boundary conditions (13) common to both the Lorentz and axial gauge, imply for the axial gauge decomposition (3) that $B\sim C\sim D/2\gg A$ throughout [12]. In this limit, the action (5) reduces to

$$S\approx\frac{3}{4\alpha}\int_{|t|<T/2}dt\int_0^\infty dx\left(\frac{1}{2}\dot{D}^2+\frac{1}{8x^2}D^4\right), \tag{15}$$

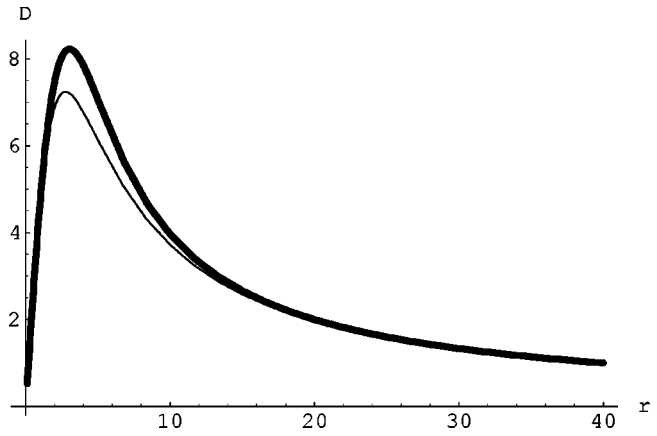

FIG. 2. $D(r,0)$ for $\rho/T=10$. See text.

the energy is

$$-\frac{Q}{M_S}\approx+\frac{3}{4\alpha}\int_0^\infty dx\left(\frac{1}{2}\dot{D}^2-\frac{1}{8x^2}D^4\right), \tag{16}$$

and the Chern-Simons number is

$$\mathbf{N}\approx\frac{1}{2\pi}\int_0^\infty dx\frac{D^3}{8x}, \tag{17}$$

with the boundary condition $D(r,\pm T/2)=-4\rho/r$. The action (15) is extremal for

$$\frac{D(r,-T/2)}{2r/(t+T/2)}=\int_1^{D(r,t)/D(r,-T/2)}\frac{dx}{\sqrt{x^4-1}}. \tag{18}$$

The transcendental equation (18) can be solved numerically. The solution is shown in Fig. 2 (thick line) for $\rho/T=10$.

A good approximation at the escape point is

$$D(r,0)\approx\frac{4\rho r}{r^2+(\sqrt{2}/K)\rho T} \tag{19}$$

which interpolates exactly between the asymptotics of the transcendental solution with $K=1.854$. Equation (18) is also shown in Fig. 2 (thin line). Its corresponding initial radial density is

$$\Theta_{00}(r,0)\approx\frac{4\pi}{g^2}\frac{24\rho^4r^2}{[r^2+(M_S/Q)^{2/5}\rho^2]^4}, \tag{20}$$

which integrates to Q. Note that the tunneling duration T relates to the energy Q through

$$\frac{T}{\rho}=\frac{K}{\sqrt{2}}\left(\frac{M_S}{Q}\right)^{2/5}. \tag{21}$$

The Chern-Simons number at the turning point for Eq. (19) is

$$\mathbf{N}=\frac{1}{2}\left(\frac{Q}{M_S}\right)^{2/5}. \tag{22}$$

At the sphaleron point with $Q=M_S$ the configuration (19) carries Chern-Simons number $\mathbf{N}=1/2$: it is a sphaleron.

For $Q>M_S$ the initial configuration follows from the sphaleron by a simple rescaling of the size ρ and the energy density,

$$\rho\to\rho/\lambda,$$
$$\Theta_{00}\to\lambda^4\Theta_{00} \tag{23}$$

with $\lambda=(Q/M_S)^{1/5}$. In Sec. V B we will evolve the gauge field configuration into Minkowski space using Luscher-Schechter (LS) solutions [14]. These solutions have a purely magnetic field configuration at $t=0$ and the (radial) energy profile

$$\Theta_{00}(r,0)=4\pi r^2\Theta_{00}(\vec{x},0)=\frac{4\pi}{g^2}\frac{48\epsilon\rho_{LS}^4 r^2}{(r^2+\rho_{LS}^2)^4}. \tag{24}$$

Comparing with the rescalings (23) we see that we have to use the LS solutions with the parameters

$$\rho_{LS}=\frac{\rho}{\lambda},$$
$$\epsilon=\frac{\lambda^4}{2}. \tag{25}$$

2. Below the sphaleron

Below the sphaleron the analytical analysis is more involved in general. For small energy Q or large times T, a perturbative expansion around the singular instanton–anti-instanton configuration has been carried out in [12]. As we will argue below, the multiplicities below the sphaleron follow from the same rescaling (23) with $Q<M_S$.

V. GLUONS IN/OUT

In this section we estimate the number of incoming (virtual) and outgoing (real) gluons present in the semiclassical singular gauge configurations for arbitrary parton-parton center of mass energy Q.

A. Incoming gluons

The number of incoming gluons follows from the exact Euclidean solutions at large Euclidean times by expanding in powers of the space Fourier transform of the large Euclidean asymptotics of the singular fields (11) as in [11,13]. In the Lorentz gauge,

$$\mathcal{A}_0^a(t,\vec{k})=2i\hat{k}_a\mathcal{Q}(\pm,k)e^{-kt},$$
$$\mathcal{A}_i^a(t,\vec{k})=-2\hat{k}_a\hat{k}_i\mathcal{Q}(\pm,k)e^{-kt}+\frac{\lambda_i^m}{\sqrt{2k}}f_a^m(\pm,k)e^{-kt} \tag{26}$$

with

$$\mathcal{Q}(\pm,k)=\frac{2\pi^2}{g}\rho^2 e^{\pm k(T/2-\rho)} \tag{27}$$

and

$$f_a^m(\pm,k)=\frac{4\pi^2\rho^2}{g}\sqrt{2k}(-\lambda_a^m+i\epsilon_{abj}\lambda_b^m\hat{k}_j)e^{\pm k(T/2-\rho)}. \tag{28}$$

The transverse polarizations are denoted by λ_a^m. In terms of the Fourier components (28) the density of incoming transverse gluons is proportional to the occupation number $\overline{aa}$ with

$$a_i^m(\theta,k)=f_i^m(+,k)e^{-k(T-\theta)/2}, \tag{29}$$

where θ is a parameter fixed by requiring the total energy of the incoming gluons to match the energy Q [11,13]. We note that T drops in the combination (29). Hence, the density of transverse gluons per unit wave number is

$$\mathbf{n}(k)=\frac{16\pi}{\alpha}\rho(k\rho)^3 e^{-4k\rho(M_S/2Q)^{1/5}}, \tag{30}$$

and the corresponding energy density per wave number is

$$\omega(k)=kn(k)=\frac{16\pi}{\alpha}(k\rho)^4 e^{-4k\rho(M_S/2Q)^{1/5}}. \tag{31}$$

Under the rescaling (23) the energy density (31) of the incoming transverse gluons follows from the sphaleron point and integrates to Q. The virtual number of gluons stripped by a sphaleron is

$$N_{\rm in}(Q)=\frac{3\pi}{8\alpha}\left(\frac{2Q}{M_S}\right)^{4/5}, \tag{32}$$

and similarly for the antisphaleron. Each virtual gluon carries in $Q/N_{\rm in}\approx\lambda$ where as before $\lambda=(Q/M_S)^{1/5}$. We recall that these gluons are absorbed from the two eikonalized partons involved in the inelastic cross section (8).

B. Outgoing gluons

To assess the number of outgoing transverse gluons produced by the singular gauge configurations in the semiclassical approximation, we need to know the gauge configurations at the escape point and their further Minkowski time evolution, much like the decay of the sphaleron in the standard model [15]. The escaping sphaleron in Minkowski space is related to an analytical solution discovered by Luscher and Schechter [14] as discussed in [10,16]. What is remarkable in our case is that through the scaling laws (23) we have tied features of this solution (energy density and multiplicity) to those of the escaping singular Yang-Mills fields above the sphaleron point.

1. At the sphaleron

The LS solution in Minkowski space at the sphaleron point is amenable to elementary functions [17] (some helpful relations can be found in the Appendices). It is strongly peaked around the light cone $t\sim r$ as it travels luminally, and for large times $t\sim r\gg\rho$ in covariant gauge it simplifies

$$A_0^a(t,v)\sim-\frac{F'}{g}n_a,$$

$$A_i^a(t,v)\sim+\frac{F'}{g}n_a n_i + \frac{F'}{gt}(v(\delta_{ai}-n_a n_i)+\rho\epsilon_{iaj}n_j) \tag{33}$$

with $v=r-t$ and

$$F'(v)=\frac{2\rho f}{\rho^2+v^2},$$

$$f(v)=\frac{1}{2}\left(1-\frac{\sqrt{2}}{\cosh(\sqrt{2}\,\xi)}\right), \tag{34}$$

and $\xi=\tan^{-1}(\rho/v)$. Note that $f(\pm\infty)=1/2-1/\sqrt{2}\sim-0.207$, with $f(0)>f(\infty)$. Choosing $F(0)=0$ we see that $F(v)$ is an odd function with asymptotics $F(\pm\infty)=\pm 0.216$. We discuss some more details of the solution in Appendix A, and show that the behavior of the gauge invariants is the same as found in [10].

Consideration of the gluon number of spectra is a more subtle issue, and should be performed in "physical" gauges. The large time asymptotics of the temporal and longitudinal gauge fields are constant at large t and proportional to $F'(v)$ with support only on the light cone. This is a gauge artifact in the covariant gauge, and can be removed by transferring to the temporal gauge by using the hedgehog gauge transformation

$$\omega(v)=e^{i\tau\cdot nF(v)} \tag{35}$$

which yields $A_0^a=0$. The temporal gauge is canonical in the sense that Gauss law is easily implemented by restricting consideration to the transverse gluons, and the vacuum state is normalizable. In this gauge the large time asymptotics of the field is purely transverse and falls as $1/t\sim 1/r$,

$$A_i^a(t,v)\sim\frac{2}{gt}\left(\sin^2F+\frac{F'}{2}[\rho\cos(2F)+v\sin(2F)]\right)\epsilon_{aij}n_j + \frac{1}{gt}(-\sin(2F)+F'[\rho\sin(2F)-v\cos(2F)]) \times(\delta_{ai}-n_a n_i). \tag{36}$$

Note that the gauge transformation (35) modifies the Chern-Simons number (7). The transverse fields in both covariant and axial gauges weaken asymptotically as $1/t$. Asymptotically the Yang-Mills solution originating from the sphaleron point Abelianizes, thereby allowing for a free wave interpretation. It is easier to carry the analysis into the covariant gauge.[4]

The large time transverse asymptotic of Eq. (33) admits a normal mode decomposition in the form

$$\mathcal{A}_i^a(t,\vec{k})=\frac{(2\pi)^{3/2}}{\sqrt{2k}}[\lambda_i^m(\vec{k})b^{am}(\vec{k})e^{-ikt} + \lambda_i^m(-\vec{k})b^{am*}(-\vec{k})e^{+ikt}] \tag{37}$$

with the λ's as the two real polarizations,

$$\lambda_i^m(\vec{k})b^{am}(\vec{k})=\frac{\rho}{g\sqrt{\pi k}}[-i\epsilon_{aij}\hat{k}_j J(k\rho) + (\delta_{ai}-\hat{k}_a\hat{k}_i)J'(k\rho)], \tag{38}$$

and

$$J(k\rho)=2\,\mathrm{Re}\int_0^{\pi/2}dy e^{ik\rho\,\mathrm{cotan}\,y}\left(1-\frac{\sqrt{2}}{\cosh(\sqrt{2}y)}\right). \tag{39}$$

The transcendental function (39) cannot be obtained in closed form, but is well behaved for $k\rho\ll 1$,

$$J(k\rho)\sim\pi-4\arctan\left[\tanh\left(\frac{\pi}{2\sqrt{2}}\right)\right], \tag{40}$$

$$J'(k\rho)\sim\pi(\sqrt{2}-1). \tag{41}$$

In terms of the normal mode decomposition (37), the asymptotic density of transverse gluons is proportional to the occupation number $|\lambda\cdot b|^2$ of the transverse modes,

$$\mathbf{n}(k)=4\pi k^2|\lambda\cdot b|^2=\frac{8\rho^2 k}{g^2}[J^2(k\rho)+J'^2(k\rho)]. \tag{42}$$

The number of gluons with small energy grows as $k\rho$, while the number of gluons with high energy falls as $k\rho e^{-2k\rho}$. The total number of prompt gluons emitted by a sphaleron is

$$N_{\mathrm{out}}(M_S)=\frac{8}{g^2}\int_0^\infty x dx[J^2(x)+J'^2(x)]=\frac{1.1}{\alpha} \tag{43}$$

where the last integration has been performed numerically.[5] The same number of gluons is produced through the anti-sphaleron. Each mode in the transverse asymptotic (37) is normal, so that the energy density carried by these modes is

[4]In the temporal gauge there is a subtlety related to the constant modes that do not admit a spectral representation. Indeed, we have checked that the space Fourier component of Eq. (36) exhibits a nonspectral term $t\,\delta(k)$.

[5]It is very similar to the spectrum obtained in the numerical analysis of [10], but different from the one discussed analytically there albeit in a different gauge, where this number was found to diverge logarithmically at small k. The occupation number is also found to diverge in the axial gauge in relation to the $k=0$ modes (see footnote 1). The gauge we use now is free from gauge artifacts.

$\omega(k)=k\mathbf{n}(k)$, which integrates to give back the sphaleron mass by energy conservation,

$$M_S=\frac{8}{g^2\rho}\int_0^\infty dx x^2[J^2(x)+J'^2(x)]=\frac{2.2}{\alpha\rho}. \tag{44}$$

The numerical result (44) is off by 7% in comparison to the exact sphaleron mass (1) which is a measure of the onset of the asymptotic normal mode expansion (37). In Appendix C we show that the expanding sphaleron configuration is stable under pair production of light quarks and gluons.

2. Away from the sphaleron by rescaling

The escape configurations above the sphaleron follow from the gauge configuration (18), (19). The latter yields the energy density of the sphaleron after the rescaling (23) and a Chern-Simons number of 1/2 at the sphaleron point. Since the electric field vanishes at the escape point, we conclude that it is very plausible that this gauge configuration is gauge equivalent to the LS gauge configuration with the parameters (25).

The analysis of the preceding section may be performed just with the substitution of $f(v)$ by

$$\frac{1}{2}[1-\sqrt{1+\sqrt{2\epsilon}}\cdot dn(\sqrt{1+\sqrt{2\epsilon}}\xi,m)] \tag{45}$$

for $\epsilon<1/2$, and by

$$\frac{1}{2}(1-\sqrt{1+\sqrt{2\epsilon}}\cdot \mathrm{cn}[(2\epsilon)^{1/4}\xi,m]) \tag{46}$$

for $\epsilon>1/2$, where

$$m=\frac{1+\sqrt{2\epsilon}}{2\sqrt{2\epsilon}}. \tag{47}$$

In Fig. 3 we show the multiplicity distributions for various values of λ. Numerically there is not much difference between the solutions obtained from the elliptic LS profiles and an appropriate rescaling (23) of the sphaleron results. In particular,

$$\mathbf{n}(k)\sim\lambda^4\frac{8k\rho^2}{g^2\lambda^2}\left[J^2\left(\frac{k\rho}{\lambda}\right)+J'^2\left(\frac{k\rho}{\lambda}\right)\right] \tag{48}$$

with $\lambda=(Q/M_S)^{1/5}$. The total number of prompt gluons emitted above the sphaleron is (in this approximation)

$$\frac{N_{\mathrm{out}}(Q)}{N_{\mathrm{out}}(M_S)}=\left(\frac{Q}{M_S}\right)^{4/5}. \tag{49}$$

The ratio of in (virtual) to out (real) gluons per sphaleron is a number independent of Q: $N_{\mathrm{in}}/N_{\mathrm{out}}\sim 2$. Prompt inelastic scattering in QCD is from few-to-few (small Q) or large-to-large gluons (large Q).

Below the sphaleron barrier, there are two turning points: $t=-T_1/2$ with zero Chern-Simons number $\mathbf{N}=\mathbf{0}$, and $t=0$ with unit Chern-Simons number $\mathbf{N}=\mathbf{1}$. The two gauge configurations and thereby multiplicities are related by the gauge transformation (13). The remarkable similarity between the scaling law (49) for the outgoing gluons above the sphaleron point and the scaling law (32) for the incoming gluons both above and below the sphaleron point leads us to *conjecture that Eq. (49) holds for the outgoing gluons below the sphaleron point as well.*

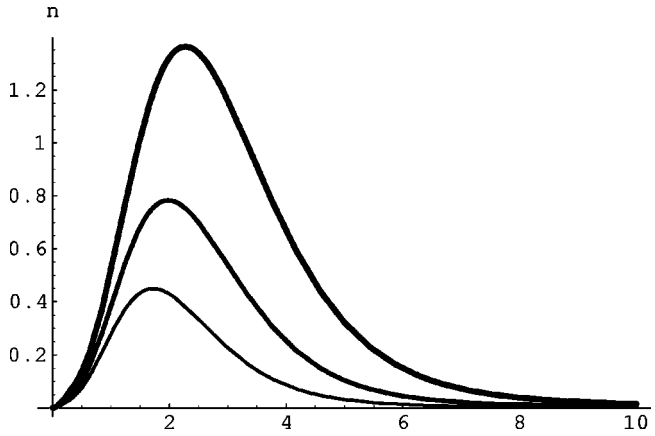

FIG. 3. Density of emitted gluons per sphaleron (multiplied by α/ρ) for $\lambda=0.5,1,2$ versus $k\rho$.

The total number of prompt gluons emitted by the escaping singular Yang-Mills configurations below the sphaleron follows the scaling law (49), which is seen to vanish at the instanton point. This result follows from a saturation of the partial cross section via classical and singular solutions to the Yang-Mills equations, and is different from the one derived recently using a minimization of the energy at the escape point by constraining the size and Chern-Simons number at the escape point [10]. The latter is likely to provide a lower bound on the partial cross section, while the former saturates it.

C. Averaging gluons

So far, we have considered the production of prompt gluons for fixed Q in the inelastic production cross section given by Eq. (8). For the singular Yang-Mills solutions considered here, the partial cross section $\sigma(Q)$ has been derived for small and large Q in [12]. In units of scaled energy $x=Q/M_S$, their result with exponential accuracy is

$$\sigma(x)=\sigma_+(x)\,\theta(x-1)+\sigma_-(x)\,\theta(1-x) \tag{50}$$

with

$$\sigma_\pm(x)=e^{(4\pi/\alpha)\mathbf{F}_\pm(x)}. \tag{51}$$

The (known part of the) holy grail function reads[6]

[6]The scaling laws derived above are specific to the energy density and the gluon multiplicities. They do not carry to the action density needed to assess the partial cross section (50) semiclassically. For that we need explicitly the escaping classical fields starting from Eqs. (18), (19) for instance.

$$\mathbf{F}_+(x) = -0.482x^{3/5},$$

$$\mathbf{F}_-(x) = -1 + 0.6185x^{4/5} - 0.0710x^{6/5} + 0.0122x^{8/5}(-\ln x + \text{const}). \quad (52)$$

The first contributions in $\mathbf{F}_\pm$ are from the semiclassical singular gauge configurations alone, while the last two contributions in $\mathbf{F}_-$ are from the one-loop and two-loop contributions, respectively [12]. The initial increase in the partial cross section in Eq. (50) follows from the rapid increase in the tunneling rate at the expense of the decrease in the matrix-element overlap. At the sphaleron point $x=1$, $\mathbf{F}_+(1) \sim \mathbf{F}_-(0)/2$, which is about half the instanton suppression factor,

$$\kappa = \sigma_+(1) \sim \sqrt{\sigma_-(0)} \sim \sqrt{e^{-4\pi/\alpha}}, \quad (53)$$

in agreement with the unitarization arguments in [5,8]. The final and rapid decrease in the cross section past the sphaleron point is caused by the decrease in the overlap between the initial and final states of the inelastic collision process.

In this subsection we would like to show that in the *inclusive gluon production* a sharp peak remains, even after we included the gluon multiplicity factor. In Fig. 4 we plot $x^{4/5}\sigma(x)$, with the typical instanton action in the QCD vacuum, $2\pi/\alpha_s(\rho) = 12$.

Using Eq. (50) we can assess the averaged number of prompt gluons produced in a parton-parton scattering process at large $\sqrt{s}$,

$$\frac{N_{\text{in,out}}(t)}{N_{\text{in,out}}} = \int_{-t/M_S^2}^{\infty} dx^2 \mu(x,t) x^{4/5} \quad (54)$$

as a function of the invariant mass transfer in the t channel, with the measure $\mu(x,t)$ fixed by the partial cross section

$$\mu(x,t) = \sigma(x) / \int_{-t/M_S^2}^{\infty} dx^2 \sigma(x). \quad (55)$$

$N_{\text{in,out}}$ are the number of gluons at the sphaleron mass. The results for the ratio (54) are displayed in Fig. 4 versus $-t/M_S^2$. The undetermined constant in Eq. (52) was adjusted to 2.418 to ensure a smooth transition at $x=1$. For $\sqrt{-t}$ within M_S, the averaged multiplicity is increased by only a factor of about 1.1 compared to the multiplicity at the sphaleron mass.

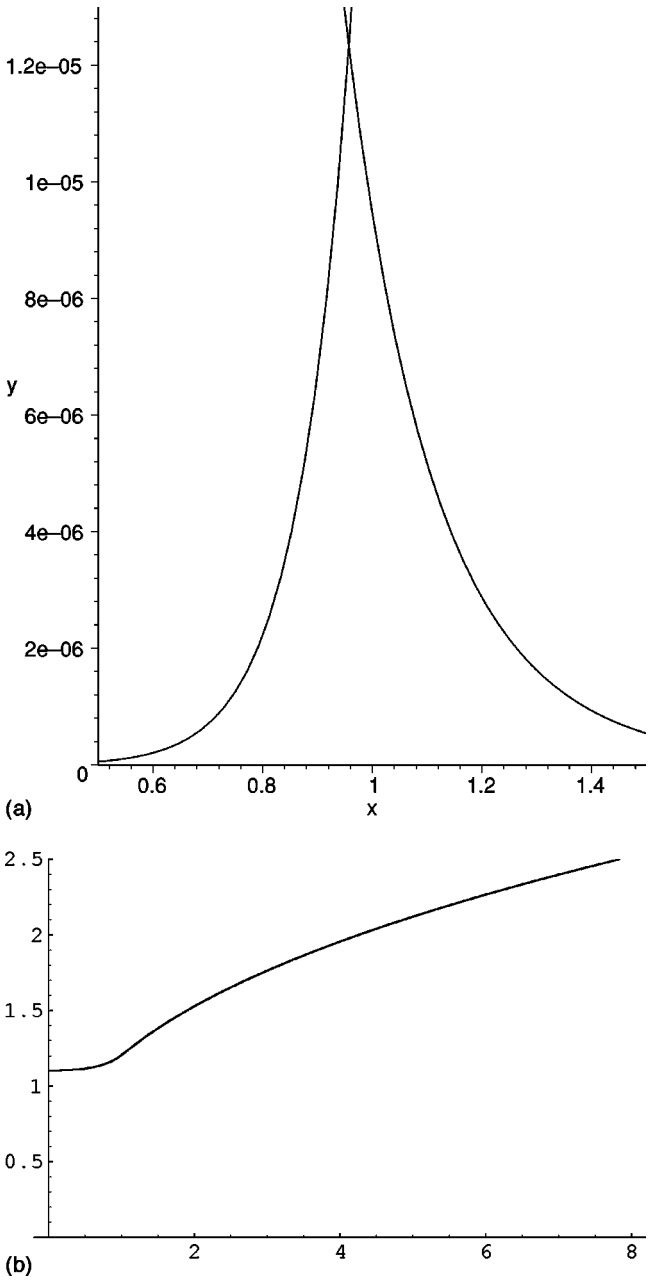

FIG. 4. (a) The inclusive gluon multiplicity $x^{4/5}\sigma(x)$ versus energy in units of the sphaleron mass $x = Q/M_S$. (b) The ratio (54) of prompt gluons emitted as a function of $-t/M_S^2$.

VI. CONCLUSIONS

The cross sections of multigluon production by instanton-induced parton-parton scattering are calculated semiclassically, using singular classical solutions of the Euclidean Yang-Mills equations. For energies Q much above the sphaleron mass we found an approximate solution which allowed us to obtain the field configuration at the turning (escape) time $t=0$. This turned out to be just a rescaled Yang-Mills sphaleron solution [10]. We also solved the Yang-Mills equations describing its Minkowski explosion at later time, which again happen to be just a rescaled version of the Luscher-Schechter solution discussed in [10]. By going to the physical gauge, we found the spectrum of the resulting gluons.

Using an analytical continuation of the singular tails into Euclidean time, we have found that the same rescaling allows for the determination of the virtual in-gluon multiplicities both above and below the sphaleron (antisphaleron) point. Thus, the in-out multiplicities at the sphaleron and antisphaleron points imply the in-out multiplicities away from this point for semiclassical parton-parton scattering. The scattering liberates about $1.1/\alpha_s(\rho)$ prompt gluons per sphaleron (antisphaleron) produced. We recall that all the calculations are semiclassical, assuming $\alpha_s(\rho) \ll 1$ or a large

produced multiplicity. The larger the longitudinal Q transferred in the c.m. frame, the smaller the size of the escaping sphaleron or antisphaleron, and vice versa. The semiclassical production through singular QCD solutions in the semihard regime may even extend to the hard regime through smaller size sphalerons. However, in this case the cross section is small. On the other hand, for typical instantons in the instanton vacuum relevant to the ''semihard'' scale and possibly the QCD Pomeron problem, this number would be about 3 gluons per cluster: thus the semiclassical analysis is not expected to be very precise.

This mechanism of gluon production is in addition to perturbative Balitskii-Fadin-Kuraev-Lipatov (BFKL) ladders and/or virtual gluon materialization in the color-glass approach [18]. The difference between this mechanism and others is seen, e.g., in the fact that the released semiclassical gluons form thin shells of a strong coherent field, which have some topological features inherited from the topological tunneling. The difference between them may be important for many applications, and is quite striking for quark production (which we address elsewhere).

We have found that the invariant mass of the gluonic cluster is sharply peaked at some (weakly energy dependent) value; one may thus ask if such phenomena have been seen experimentally. It is known from correlation measurements that multiparticle production in pp collisions is dominated by some clusters or clans: for a recent discussion see, e.g., [20]. The multiplicity per cluster is slowly growing with energy. The invariant mass is unknown since neutrals are not seen, but happens to be in the pertinent range of a few MeV. In a calorimeter study of double diffractive events by the UA8 Collaboration [19], a single cluster was produced and its invariant mass was measured and found to be peaked around 3 GeV, with a strongly decreasing tail at larger mass. Moreover, the clusters with mass less than 5 GeV show remarkable spherical decays (in their rest frame). We are currently investigating specific decay modes and evaluating their relevant cross sections to see whether the qualitative agreement with the present work can be made more quantitative.

ACKNOWLEDGMENTS

This work was supported in part by the U.S. DOE grant DE-FG-88ER40388. R.J. was supported in part by KBN grants 2P03B01917 and 2P03B09622.

APPENDIX A: LS SOLUTION

In this section we give a brief characterization of the LS gauge configuration. The reader is also referred to [17] for more details. For the Euclidean Witten ansatz

$$-eA_0^a=\frac{x_a}{r}A_0, \tag{A1}$$

$$-eA_i^a=\varepsilon_{ian}\frac{x_n}{r^2}(1+\phi_2) + \frac{x_a x_i}{r^2}A_1+\left(\delta_{ai}-\frac{x_a x_i}{r^2}\right)\frac{\phi_1}{r}. \tag{A2}$$

The coefficient functions for the LS solutions continued to Euclidean space are

$$A_0=-4q_{LS}\gamma^2 rt, \tag{A3}$$

$$A_1=-4q_{LS}\gamma^2\frac{1+r^2-t^2}{2}, \tag{A4}$$

$$\phi_1=-4q_{LS}\gamma^2 r\frac{1-r^2-t^2}{2}, \tag{A5}$$

$$\phi_2=-4q_{LS}\gamma^2 r^2-1, \tag{A6}$$

$$\gamma^2=\frac{1}{(1-r^2-t^2)^2+4r^2}, \tag{A7}$$

and q_{LS} is a function of $\operatorname{arctanh}[2t/(1+r^2+t^2)]$.

In terms of these quantities the electric and magnetic fields are given by formula[7] (7.27) in [17]. We perform the calculations for the sphaleron point which corresponds to

$$q_{LS}=-1+\frac{\sqrt{2}}{\cos\{\sqrt{2}\,\operatorname{arctanh}[2t/(1+r^2+t^2)]\}}. \tag{A8}$$

We rotate these formulas back to Minkowski space using $t\to it$. The solutions are again concentrated on the light cone. We perform then the limit $t\to\infty$ keeping $v=r-t$ fixed. The results for the ''electric'' coefficients of formula (7.27) in [17] are

$$D_0\phi_2/r\to\frac{v+2\ \operatorname{sech}^2 u(\sinh u-v)}{t(1+v^2)^2}, \tag{A9}$$

$$F_{01}\to\frac{1}{t}\cdot 0, \tag{A10}$$

$$D_0\phi_1/r\to\frac{1-2\ \operatorname{sech}^2 u(v\sinh u+1)}{t(1+v^2)^2}, \tag{A11}$$

where $u\equiv\sqrt{2}\ \operatorname{arctanh}(1/v)$. The ''magnetic'' coefficients are

$$-D_1\phi_1/r\to i\frac{1-2\ \operatorname{sech}^2 u(v\sinh u+1)}{t(1+v^2)^2}, \tag{A12}$$

[7] In the original formula (7.27) the coefficient of F_{01} is off by a factor of r^2.

$$(1-\phi_1^2-\phi_2^2)/r^2 \to \frac{1}{t}\cdot 0, \tag{A13}$$

$$D_1\phi_2/r \to -i\frac{v+2\ \ \mathrm{sech}^2 u(\sinh u - v)}{t(1+v^2)^2}. \tag{A14}$$

For large times t, the electric and magnetic fields are equal,

$$\vec{E}^2(t,v) \sim \vec{B}^2(t,v) \sim \frac{2}{t^2}\frac{1}{(1+v^2)^3}, \tag{A15}$$

and sum up to M_S. The same result was obtained in [10].

The ''antisphaleron'' follows from the sphaleron by substituting

$$A_0 \to -A_0, \tag{A16}$$

$$A_1 \to -A_1, \tag{A17}$$

$$\phi_1 \to -\phi_1, \tag{A18}$$

$$\phi_2 \to \phi_2 \tag{A19}$$

in the Witten ansatz above, and yields a solution of the YM equation of motion. The same transformation makes a switch between the instanton and anti-instanton in the Witten ansatz.

APPENDIX B: Im S FOR LS SOLUTION

In this appendix we will show that the imaginary part of the classical action along the deformed contour [16] does not depend on the energy of the LS solution. In other words, the instanton–anti-instanton suppression factor persits all the way to the sphaleron point in the deformed contour approach suggested in [16]. Indeed, for $\varepsilon < 1/2$ the solution is given by the function

$$q = q_- \mathrm{sn}(q_+\phi + K, k) \tag{B1}$$

where we use the same notation as in [16],

$$q_\pm = \sqrt{1 \pm \sqrt{2\varepsilon}}, \quad k^2 = \frac{q_-^2}{q_+^2}, \tag{B2}$$

and

$$\phi = \mathrm{arccoth}\left(\frac{1+r^2+\tau^2}{2\tau}\right). \tag{B3}$$

The suppression factor is given by

$$\mathrm{Im}\, S = -\frac{24\pi^2}{g^2}\int_0^\infty dr\ \mathrm{Im}\sum_{nm}\ \mathrm{Res}\left\{\frac{\cos^4 w}{r^2}\mathcal{E}\right\} \tag{B4}$$

where

$$\mathcal{E} \equiv \frac{1}{2}\dot{q}^2 + \frac{1}{2}(q^2-1)^2. \tag{B5}$$

The residues are calculated at the poles of Eq. (B1) inside the contour. One can show that $\mathcal{E}$ is just equal to $(q^2-1)^2-\varepsilon$. We will now use the Laurent expansion of the elliptic sine

$$\mathrm{sn}(u) \sim \frac{\alpha}{u-u_0} + \beta(u-u_0). \tag{B6}$$

Using the differential equation for $\mathrm{sn}(u)$ we obtain the relations $\alpha^2 k^2 = 1$ and $\beta = (\alpha/6)(1+k^2)$. We thus have to compute

$$\mathrm{Res}(\cos^4 w\mathcal{E}) = \alpha^4 k^4\,\mathrm{Res}\left(\frac{\cos^4 w}{(\phi-\phi_0)^4}\right) + (4\alpha^3\beta k^2 q_-^2 - 2\alpha^2 k^2)\,\mathrm{Res}\left(\frac{\cos^4 w}{(\phi-\phi_0)^2}\right). \tag{B7}$$

The coefficients of the residues are energy independent and equal to 1 and $-2/3$, respectively. Once we use

$$\cos^2 w \equiv \frac{4r^2}{(1+r^2)^2 + 2\tau^2(r^2-1) + \tau^4} \tag{B8}$$

and the r dependence of the poles $\tau(r) = q + \sqrt{q^2-1-r^2}$ where q is an ε dependent constant, we obtain

$$\int_0^\infty \frac{dr}{r^2}\mathrm{Res}\left(\frac{\cos^4 w}{(\phi-\phi_0)^4}\right) = \frac{i}{3}\frac{1+q^2}{1-q^2}, \tag{B9}$$

$$\int_0^\infty \frac{dr}{r^2}\mathrm{Res}\left(\frac{\cos^4 w}{(\phi-\phi_0)^2}\right) = i\frac{1}{1-q^2}. \tag{B10}$$

Finally, we get

$$\mathrm{Im}\, S = \frac{8\pi^2}{g^2}. \tag{B11}$$

Note that the whole energy dependence through ε has canceled out.

APPENDIX C: STABILITY UNDER PAIR DECAY

Are the escaping Yang-Mills fields stable under pair decay? In this appendix, we answer this question by assessing the gluon or quark pair emission rate in a general time dependent background to first order in α. Let $\mathcal{T}(A)$ be the on-shell matrix element between a particle and an antiparticle in the external gauge field. Typically, the number of pairs per unit four-volume is

$$\frac{dN_{q\bar{q}}}{d^4x} = \mathrm{Tr}\langle x|\ln[\mathbf{1} - \mathcal{T}(A)\mathbf{P}(+)\overline{\mathcal{T}}(A)\mathbf{P}(-)]|x\rangle \tag{C1}$$

where $\mathbf{P}(\pm)$ are the on-shell projectors on particles and antiparticles, and the trace is over color and spin. In the momentum representation

$$\mathbf{P}(\pm)=2\pi(\not{P}+m_F)\,\theta(\pm P_0)\,\delta(P^2-m_F^2) \tag{C2}$$

for a flavor of mass m_F. Since the pair creation follows from large times (weak fields), we may approximate $\mathcal{T}(A)$ by its leading order

$$\mathcal{T}(A)\approx ig\not{A}. \tag{C3}$$

Inserting Eq. (C3) into Eq. (C1), expanding the logarithm, integrating over all space-time, and insisting on gauge invariance yield the pair rate

$$\frac{dN_{qq}^{-}}{d^4q}=\frac{\mathbf{4}\alpha}{12(2\pi)^4}(|\mathbf{E}_i^a(q)|^2-|\mathbf{B}_i^a(q)|^2) \times\theta(q^2-4m_F^2)(1-4m_F^2/q^2)^{1/2}(1+2m_F^2/q^2), \tag{C4}$$

where $(\mathbf{E},\mathbf{B})$ are the Fourier transforms of the chromoelectric and -magnetic fields in Minkowski space,

$$(\mathbf{E},\mathbf{B})(q)=\int d^4x e^{iq\cdot x}(\mathbf{E},\mathbf{B})(x). \tag{C5}$$

We have highlighted **4** in Eq. (C4) to show

$$\mathbf{4}=\frac{1}{2}\times 2\times 2\times 2 \tag{C6}$$

for $g/\sqrt{2}$ fundamental quark charge, two flavors, two spins, and two particle-antiparticles, respectively. Notice that the production in Eq. (C4) is timelike, for which $q=(\omega,\vec{0})$ is an allowed frame. Such frames support zero magnetic fields, indicating that the pair production mechanism is electric in nature. It is of order α^0 in the strong coupling constant. In deriving Eq. (C5) we have ignored the back reaction of the quarks on the YM fields.

Since the $\bar{u}u$ and $\bar{d}d$ pairs are light, we may set $m_F\approx 0$ in Eq. (C4). The total number of light quark pairs emitted by the classical field is

$$N_{\bar{u}u+\bar{d}d}^{-}=\frac{\alpha}{3(2\pi)^4}\int d^4q\,\theta(q^2)(|\mathbf{E}_i^a(q)|^2-|\mathbf{B}_i^a(q)|^2). \tag{C7}$$

The present arguments can also be used to derive a similar expression for the number of gluon pairs emitted by the classical field in the weak field limit. For $N_c=3$, the gluons can be organized in three conjugate pairs, such as W^+W^-, K^+K^-, K^0K^0, by analogy with the charged octet mesons. Say we choose the external field to be K^0; then K^0 may decay into the two charged modes W^+W^- and K^+K^-. Using the background field method, the result for the two-gluon multiplicity is

$$N_{gg}=\frac{\mathbf{3}\alpha}{12(2\pi)^4}\int d^4q\,\theta(q^2)(|\mathbf{E}_i^a(q)|^2-|\mathbf{B}_i^a(q)|^2). \tag{C8}$$

We have highlighted **3**,

$$\mathbf{3}=\frac{3}{4}\times 2\times 2, \tag{C9}$$

for $g\sqrt{3}/2$ charge, two decay modes, and two physical helicities, respectively. Combining Eq. (C7) with Eq. (C8) we find that the light quark and gluon multiplicities are related by

$$N_{\bar{u}u+\bar{d}d}^{-}=\frac{2N_F}{3}N_{gg}. \tag{C10}$$

Using the results of Appendix B, we find

$$\int d^4q\,\theta(q^2)(|\mathbf{E}_i^a(q)|^2-|\mathbf{B}_i^a(q)|^2)=0. \tag{C11}$$

The expanding sphaleron starts magnetic and remains magneticlike throughout. It is stable under light-pair quantum emission.

[1] A. A. Belavin, A. M. Polyakov, A. S. Schwarts, and Y. S. Tyupkin, Phys. Lett. **59B**, 85 (1975).
[2] G. 't Hooft, Phys. Rev. D **14**, 3432 (1976); **18**, 2199 (1978).
[3] T. Schafer and E. V. Shuryak, Rev. Mod. Phys. **70**, 323 (1998).
[4] A. Ringwald, Nucl. Phys. **B330**, 1 (1990); O. Espinosa, *ibid.* **B343**, 310 (1990); V. V. Khoze and A. Ringwald, Phys. Lett. B **259**, 106 (1991).
[5] V. I. Zakharov, Nucl. Phys. **B353**, 683 (1991).
[6] M. Maggiore and M. Shifman, Phys. Rev. D **46**, 3550 (1992).
[7] A. Ringwald and F. Schrempp, Phys. Lett. B **503**, 331 (2001); F. Schrempp, J. Phys. G **28**, 915 (2002).
[8] E. Shuryak and I. Zahed, Phys. Rev. D **62**, 085014 (2000); M. Nowak, E. Shuryak, and I. Zahed, *ibid.* **64**, 034008 (2001).
[9] D. Kharzeev, Y. Kovchegov, and E. Levin, Nucl. Phys. **A690**, 621 (2001).
[10] D. Ostrovsky, G. Carter, and E. Shuryak, Phys. Rev. D **66**, 036004 (2002).
[11] S. Khlebnikov, Phys. Lett. B **282**, 459 (1992).
[12] D. Diakonov and V. Petrov, Phys. Rev. D **50**, 266 (1994).
[13] S. Khlebnikov, V. Rubakov, and P. Tinyakov, Nucl. Phys. **B350**, 441 (1991).
[14] M. Luscher, Phys. Lett. **70B**, 321 (1977); B. Schechter, Phys. Rev. D **16**, 3015 (1977).
[15] M. Hellmund and J. Kripfganz, Nucl. Phys. **B373**, 749 (1991); J. Zadrozny, Phys. Lett. B **284**, 88 (1992); D. Diakonov and M. Polyakov, Phys. Rev. D **49**, 6864 (1994); J. Schaldach, P. Sieber, D. Diakonov, and K. Goeke, *ibid.* **54**, 2814 (1996).

[16] T. Gould and E. Poppitz, Nucl. Phys. **B418**, 131 (1994); D. Son and P. Tinyakov, *ibid.* **B415**, 101 (1994).
[17] A. Actor, Rev. Mod. Phys. **51**, 461 (1979).
[18] L. McLerran and R. Venugopalan, Phys. Rev. D **49**, 2233 (1994); **49**, 3352 (1994).
[19] UA8 Collaboration, A. Brandt *et al.*, Eur. Phys. J. C **25**, 361 (2002).
[20] A. Giovannini and R. Ugoccioni, hep-ph/0209040.